Direct Depiction of Bone Microstructure Using ZTE Imaging

M. Weiger[1,2], M. Stampanoni[3,4], and K. P. Pruessmann[3]
[1]Bruker BioSpin AG, Faellanden, Switzerland, [2]Bruker BioSpin MRI GmbH, Faellanden, Germany, [3]Institute for Biomedical Engineering, University and ETH Zurich, Zurich, Switzerland, [4]Swiss Light Source, Paul Scherrer Institute, Villigen, Switzerland

Introduction In most MR images, bone appears dark due to its relatively low water content with very short transverse relaxation times of a few hundreds of microseconds. Therefore, on a macroscopic scale, MRI of bone is usually based on contrast to adjacent tissue or signal from embedded bone marrow, which exhibits larger proton density and longer T_2. Only with techniques that capture and encode MR signal immediately after excitation, like UTE [1] or WASPI [2], bone tissue can be visualised directly. In bone research and diagnostics, there is also strong interest in depicting the structure of cortical and trabecular bone on a microscopic scale [3]. This has been accomplished by micro-computed tomography (µCT) [4, 5], synchrotron-based x-ray tomographic microscopy (SRXTM) [6, 7], as well as micro-MRI (µMRI) [8-10]. In the µMRI approaches, bone is again not imaged directly but in contrast to adjacent material, which is either the bone marrow [8] or some fluid replacing the latter in in-vitro studies [9, 10]. Direct depiction of bone microstructure has so far been hampered by the difficulty of achieving very high resolution and SNR efficiency under the rapid T_2 relaxation of bone. In the present work, it is proposed to improve this capability with ZTE imaging, which combines zero echo time with maximum encoding speed in the *k*-space centre and a high acquisition duty cycle. It is shown that this approach permits the direct mapping of trabecular micro-architecture, which is verified by additional SRXTM imaging.

Methods *µMRI:* In ZTE, 3D radial centre-out *k*-space encoding is employed, while zero TE is achieved by switching on the readout gradient before RF excitation by a large-bandwidth hard pulse [11, 12] (Fig. 1). The data obtained in this manner is incomplete around the *k*-space centre due to finite pulse duration, transmit-receive (T/R) switching, and digital filter build-up. Images without baseline artefacts can nevertheless be obtained by algebraic reconstruction based on radial acquisition oversampling and finite support extrapolation [13, 14]. ZTE was performed on a Bruker µMRI-system equipped with a 7 T vertical standard-bore magnet, an AVII console, a Micro5 probe head, a gradient system with a maximum strength of 288 G/cm, and an RF saddle coil with 5 mm diameter and 20 mm length. The imaging parameters were: resolution (56 µm)^3, matrix size 144^3, flip angle 4°, TR 1.5 ms, 65619 radial readouts, 2120 averages, resulting in a total scan time of 58 h. The sequence timing was based on a signal bandwidth of 200 kHz and involved the dwell time dw = 5 µs, readout duration 360 µs, acquisition oversampling 4, T/R switching duration 4.5 µs, RF pulse duration 1 µs, creating a dead time Δ = 1.375 dw. *SRXTM:* Data were acquired at the TOMCAT beamline of the Swiss Light Source, using a matrix size of 2048^2 × 1780 and a pixel size of (1.85 µm)^3 [15]. The scan time was 5 minutes at an x-ray energy of 17.5 keV. *Sample:* A piece of about (4 mm)^3 of trabecular bone was extracted from a bovine joint and dried under ambient conditions for about 6 months. *Processing:* The SRXTM data were down-sampled by a factor of 4 for easier handling. The two data sets were co-registered manually by allowing translational and rotational degrees of freedom.

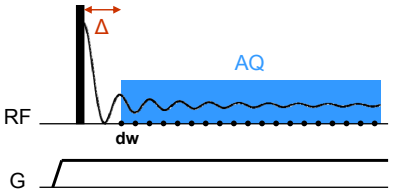

Figure 1 *ZTE acquisition scheme with dwell time* dw *and dead time* Δ.

Results Figure 2 shows one axial and two longitudinal slices from the µMRI data, the SRXTM data, and an overlay of the two. The µMRI slices are displayed with bilinear interpolation, whereas the SRXTM images are maximum-intensity projections over the MRI slice thickness. In the µMRI images, the trabecular micro-architecture is well depicted with a medium signal level for the bone matrix. Marrow appears brighter due to higher proton density whereas large parts of the marrow spaces are empty due to shrinkage. Despite the lipid chemical shift of about 1000 Hz, only minor blurring is observed owing to the large acquisition bandwidth. Similarly, no strong off-resonance artefacts occur at interfaces to the surrounding air. The indicated bright artefact arises from a contamination in the probe located in the non-linear range of the gradients, which gave off a very short-T_2 proton signal. After registration with the SRXTM images, the depiction of both bone and marrow shows excellent agreement between the two modalities.

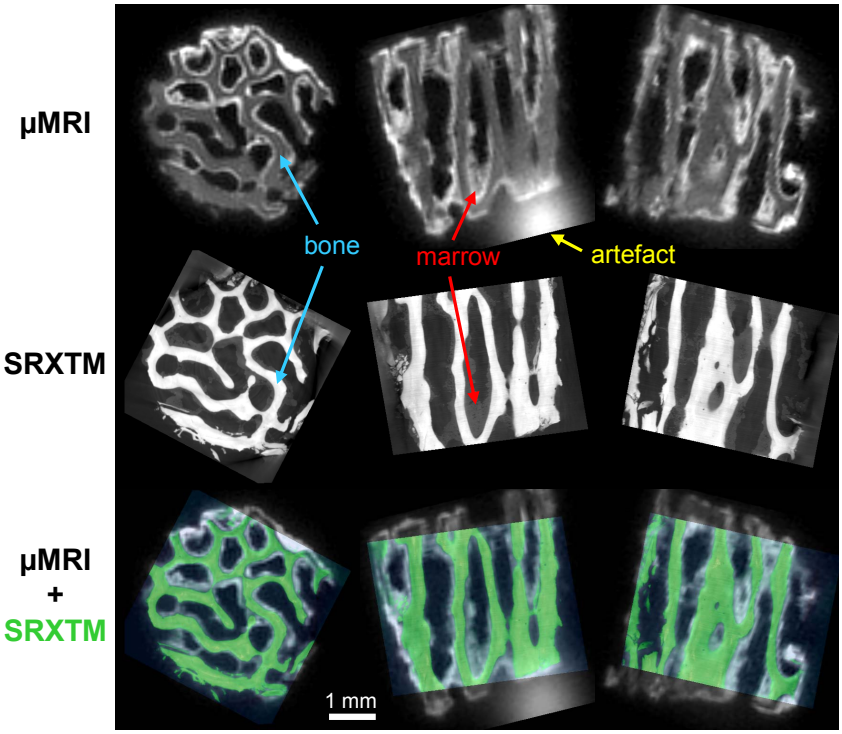

Figure 2 *ZTE imaging of trabecular bone microstructure at an isotropic resolution of resolution 56 µm in comparison with synchrotron-based x-ray tomography.*

Discussion It has been demonstrated that the microstructure of trabecular bone can be depicted directly by MRI with zero echo time, relying on its particular ability to capture and spatially encode MR signal with very short T_2. The associated high bandwidth also makes the ZTE technique robust against off-resonance artefacts related to chemical shift or tissue-air interfaces. Unlike previous approaches that target negative contrast, no defined filling or other preparation of the sample is required. Furthermore, the ability to observe signal changes in the bone tissue itself might provide information about physiological and pathological conditions. Hence, while inferior to x-ray techniques in terms of spatial resolution and SNR, short-T_2 µMRI can possibly provide useful complementary information in bone studies. To this end, additional contrast mechanisms for ZTE, such as preparation pulses in segmented schemes, are still to be explored. The long scan times inherent to MR microscopy can likely be somewhat reduced by specialized RF coil hardware. Moreover, higher water content is expected in fresh bone, thus providing larger signal and requiring less averaging.

References [1] Gatehouse PD, MRI 22 (2004) 1061. [2] Wu Y, MRM 57 (2007) 59. [3] Sornay-Rendu E, J Bone Miner Res 2 (2007) 425. [4] Majumdar S, Osteoporosis Int 6 (1996) 376. [5] Boutroy S, J Clin Endicrinol Metab 90 (2005) 6508. [6] Schneider P, Microsc Res Tech 72 (2009) 690. [7] Schneider P, J Bone Miner Res, 22 (2007) 1557 [8] Jara H, MRM 29 (1993) 528. [9] Chung HW, J Bone Miner Res 10 (1995) 1452. [10] Palombarini M, JMRI 30 (2009) 825. [11] Hafner S, MRI 12 (1994) 1047. [12] Weiger M, ISMRM 2010, 695. [13] Jackson J, MRM 11 (1989) 248. [14] Kuethe DO, JMR 139 (1999) 18. [15] Stampanoni M, in: Developments in x-ray tomography V, Proc. SPIE 6318 (2006) 63180M.